8/15/78 FERMILAB-CONF-78-120-E
Submitted to the XIX International Conference on High Energy Physics, Tokyo, Japan, 1978.

A High Statistics Study of Dimuon Production by 400 GeV/c Protons*

S. Childress[1], D. Garelick[2], P. Gauthier[2], M. Glaubman[2], H.R. Gustafson[3], H. Johnstad[2], L. Jones[3], M. Longo[3], M. Mallary[2], P. Mockett[1], J. Moromisato[2], W. Oliver[4], T. Roberts[3], J. Rutherfoord[1], S. Smith[1], E. von Goeler[2], M. Whalley[3], R. Weinstein[2], and R. Williams[1]

---

*This work was supported in part by the National Science Foundation and the U.S. Department of Energy.

[1] Department of Physics, University of Washington, Seattle, Washington 98195

[2] Department of Physics, Northeastern University, Boston, Massachusetts 02115

[3] Department of Physics, University of Michigan, Ann Arbor, Michigan 48104

[4] Department of Physics, Tufts University, Medford, Massachusetts 02155

ABSTRACT

The mass, p_T, x_F, and $\cos\theta^*$ dependences of $\mu^+\mu^-$ production by 400 GeV protons on a Tungsten target are reported. The data sample contains 275,000 events with $M_{\mu\mu} \geq 6$ GeV and has ~15,000 $T \rightarrow \mu^+\mu^-$ events.

Introduction:

We report here preliminary results of a high statistics study of $\mu^+\mu^-$ production by 400 GeV protons on a Tungsten target carried out at the Fermi National Accelerator Laboratory. Some details of the apparatus and earlier results can be found in References 1 and 2 (attached). This paper is divided into three sections. Section I discusses the analysis techniques. In Section II, the mass spectrum is presented and discussed. Feynman x, p_T and $\cos\theta^*$ distributions as a function of mass are presented in Section III.

Section I: Analysis Techniques

The basic technique used is to generate events using Monte Carlo (MC) techniques and an assumed physics model and to compare the MC generated event distributions to the actual data. The MC generation takes into account essentially all known properties of the apparatus. For example, multiple scattering and energy loss of the muons, detector spacial resolution, the beam phase space and attenuation in the target, and the exact geometry of the detector.

The physics model used for the MC generation is:

$$(1) \qquad \frac{d\sigma}{dM_{\mu\mu}dx_F dp_T^2 d\cos\theta^*} = \frac{C(1-|x_F|)^n (1+\alpha\cos^2\theta^*) e^{-aM_{\mu\mu}}}{\left[1+\left(\frac{p_T}{p_o}\right)^2\right]^6}$$

where the quantities C, n, p_o, α, and a were adjusted to reproduce the data reasonably well. Here x_F is the Feynman x and p_T is the transverse momentum of the mu-pair. The decay polar angle in the mu-pair center-of-mass, θ^*, is with respect to the "quark-quark" frame.[3] In general, the quantities C, n, p_o, α, and a can depend on the kinematic variables. The final determination of these quantities from the data are discussed in Sections II and III.

Section II: The Mass Spectrum

Figure 1 shows the mass acceptance of our detector when the trigger was set to reject low mass events. Virtually all of our high mass data was taken with this trigger. For acceptance calculations the MC program assumed n=3, p_o=2.8GeV, α=0, and a=1.0. The lower points show the geometric acceptance in the usual sense. The upper curve is the one we use to correct the data and includes a correction for resolution smearing which is important at higher masses. Figure 2 shows the MC calculated r.m.s. fractional mass resolution ($\Delta M_{\mu\mu}/M_{\mu\mu}$) as a function of mass. The lower points show the resolution limit due to the finite MWPC wire spacing. The rest is due almost entirely to multiple scattering of the muons in the solid iron magnets.

Figure 3 shows the uncorrected yield graphed versus mass and summed over the other kinematic variables. The level of backgrounds from uncorrelated pairs of muons can be inferred by studying those triggers which contain two like-sign muons. The lower data points, representing such pairs, have been

corrected for the fact that the acceptance for like-sign pairs is different from that for the opposite-sign pairs. By studying triggers with one muon out of time with the second, we conclude that our like-sign spectrum is dominated by accidentals. Such backgrounds appear to be negligably small except at the lowest masses.

The acceptance corrected mass spectrum is displayed in Figure 4. The long region of smooth fall off of the continuum both above and below the T region makes the T signal stand out well. This spectrum was fit with the form in equation 2:

$$(2)\quad Y(M_{\mu\mu}) = A_c e^{-(aM_{\mu\mu}+bM_{\mu\mu}^2)} + A_r G(M_r,\sigma_r)$$

where $G(M_r, \sigma_r) = \frac{\Delta M}{\sqrt{2\pi}\,\sigma_r} e^{-(M_{\mu\mu}-M_r)^2/2\sigma_r^2}$

and ΔM is the bin width. The normalization is chosen so that A_r gives the number of events in the Gaussian shaped resonance. Multiplying A_r by the full acceptance gives the actual number of $T \to \mu^+\mu^-$ events recorded by this experiment. All parameters in the fit were allowed to vary without constraint. The results are summarized in Table I. The fit gives values for M_r in good agreement with the mass of the T given in references 4-7.

As is evident in Figure 5, there is no apparent structure in the mass spectrum above the T region.

Section III: Production Dynamics

Three mass intervals are indicated at the bottom of Figure 5. Mass intervals numbered 1 and 3 (designated M_1 and M_3 for short) contain the continuum below and above the T region respectively. Region M_2 also has some continuum but approximately 40% of this data is from the T. In this section we will present preliminary results from fits to the x_F, p_T and $\cos\theta^*$ distributions.

The acceptance in p_T (including resolution smearing effects as discussed for Figure 1) integrated over x_F for each mass interval is presented in Figure 7. Figure 8 shows the results of three Monte Carlo's in the M_2 mass range. The highest set of data shows our best parameterization with all known apparatus effects folded in. The data in the middle is the same except that the detector resolution is not folded in. The lowest data set shows what our data would look like if all dimuons had $p_T=0$, i.e. it is the resolution function. Each data set is independently normalized.

We have further subdivided the data into three intervals of x_F and show in Figure 9 the fitted value of p_o using the parameterization of Equation 1. The circles show the results of fits using the data in the range $0.<p_T<4.0$ GeV. The errors are dominated by systematic uncertainty in the acceptance. Some QCD calculations[10] have suggested that the p_T distribution should become narrower as x_F increases. Our data is inconsistent with this prediction. For more detailed comparison with QCD

predictions we have also fit the same data only above p_T = 1.0 GeV. No systematic change in this conclusion is evident.

The data, integrated over x_F, is graphed versus $M_{\mu\mu}$ in Figure 10. This data is quite consistent with that of Yoh, et.al.[7]

One of the unique features of this experiment is the broad acceptance in x_F. The resolution smeared acceptance function for the M_2 mass interval is shown in Figure 11. Also shown is the resolution function at $x_F = 0$ and $x_F = 0.7$. As can be seen from the acceptance corrected data, the functional form $(1-|x_f|)^n$ is not a particularly good representation of the data. A definite asymmetry about $x_F = 0$ is apparent and is expected because of the neutron content of the Tungsten target. Nevertheless, the parameter n is a sensitive indication of the general shape of the x_F distributions. Figure 12 shows how this shape parameter changes with mass.

Our acceptance in $\cos\theta^*$, shown in Figure 13, is not wide enough to obtain data of sufficient precision to test current models. Figure 14 shows the result of fits to the data of the form $1+\alpha\cos^2\theta^*$ for the three mass intervals.

We wish to thank J. Gallagher, M. El-Rayess, E. Kaiser, R. Spielmaker, D.Logothetis, and the Fermilab Directorate and staff for considerable help and encouragement.

Footnotes and References

1. D. A. Garelick, et al., Northeastern University Preprint NUB #2348, To be published in Phys. Rev. D, September 1, 1978.
2. W. P. Oliver, et al., Tufts Preprint No: TUFTSPUB 78-1601. Submitted to Proceedings of the 3rd International Conference at Vanderbilt University on New Results in High Energy Physics.
3. We define $\cos\theta^* = (p_L^+ - p_L^-)/(p_L^+ + p_L^-)$ where $p_L^+(p_L^-)$ is the longitudinal momentum of the $\mu^+(\mu^-)$ in the laboratory.
4. S. W. Herb, et al., Phys. Rev. Lett. 39, 252 (77).
5. W. R. Innes, et al., Phys. Rev. Lett. 39, 1240 (77).
6. D. M. Kaplan, et al., Phys. Rev. Lett. 40, 435 (78).
7. J. K. Yoh, et al., FERMILAB-Pub-78/52-EXP 7180.288, submitted to Phys. Rev. Lett.
8. Pluto Collaboration (Ch. Berger, et al.) DESY 78/21 (to be published in Phys. Lett. B)
9. C. W. Darden, et al., DESY 78/22 (to be published in Phys. Lett. B)
10. F. Halzen and D. M. Scott, University of Wisconsin Preprint, COO-881-37 (1978).

    Edmond L. Berger, Argonne Preprint ANL-NEP-PR-78-12 (1978). To be published in the Proceedings of the 3rd International Conference at Vanderbilt University on New Results in High Energy Physics.

TABLE I

Results of fit to mass spectrum. Fit region is 7.0<M<15.0 GeV.

$a = 1.12 \pm 0.06\ \text{GeV}^{-1}$

$b = -0.007 \pm 0.003\ \text{GeV}^{-2}$

$A_r \times \text{Acceptance} = 14660 \pm 1340$ events

$M_r = 9.52 \pm 0.06$ GeV

$\sigma_r = 0.92 \pm 0.04$ GeV

$(\sigma_{MC}\ (M_{\mu\mu} = 9.5\ \text{GeV}) = 0.61)$

$$R = \frac{B\ \sigma(T)}{\frac{d\sigma}{dM_{\mu\mu}}\ (M_{\mu\mu} = 9.5\ \text{GeV})} = 1.18 \pm 0.11\ \text{GeV}$$

$\chi^2/\text{d.f.} = 58.2/34$

Figure Captions

1. Mass acceptance for this experiment. The data points show the Monte Carlo calculated geometric acceptance. The upper curve shows the acceptance including effects of resolution smearing.
2. The r.m.s. fractional mass resolution $\Delta M_{\mu\mu}/M_{\mu\mu}$. The lower data points show the resolution limit due to the finite wire spacing of the MWPC's. The resolution is dominated by multiple scattering in the solid iron magnets.
3. Yield of dimuons as a function of $M_{\mu\mu}$ before acceptance corrections. The like sign pairs have been corrected for the difference in acceptance between them and the opposite sign pairs.
4. Corrected mass spectrum.
5. A fit to the mass spectrum. See text.
6. The Υ signal after subtraction of the continuum fit of Figure 5.
7. Resolution smeared acceptance corrections for the p_T data for the three mass regions shown in Figure 5.
8. Three MC's versus p_T. The upper data is the full simulation, the middle is the full simulation but without resolution folded in, and the lower data is the resolution function.

9. Results of fits to the p_T data. For definition of the parameter p_o see equation 1. The circles are the result of the fit including data in the range $0 \leq p_T \leq 4$ GeV. The triangles are for $1 \leq p_T \leq 4$ GeV for better comparison to QCD calculations. See Reference 10. For plotting purposes the triangles have been displaced by $\Delta x_F = +0.03$ from their true values.

10. The parameter p_o averaged over all x_F.

11. This figure includes the resolution smeared acceptance correction, the corrected data, the resolution function at 0. and .7 and the parameterization $(1-|x_F|)^{3.0}$ for the data in the M_2 interval versus x_F.

12. The result of the fitting parameter n to the x_F data versus $M_{\mu\mu}$.

13. Data in the M_3 mass interval versus $\cos\theta^*$ after the acceptance correction which is also shown. The resolution function is also shown and is relatively constant over the whole $\cos\theta^*$ range. The curve is the result of a fit of the form $1+\alpha\cos^2\theta^*$.

14. The fitting parameter α for the three mass intervals.

FIG. 1

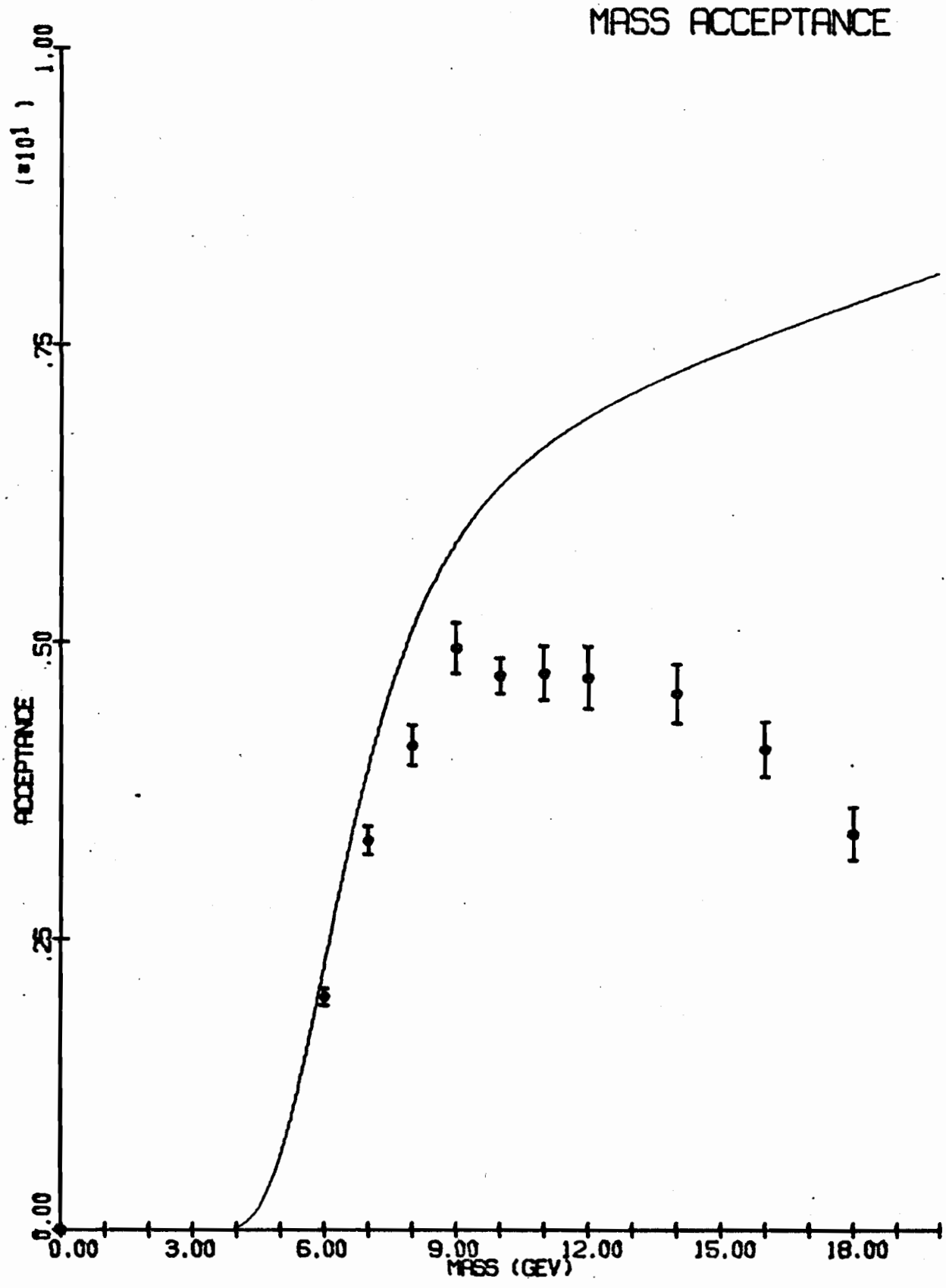
MASS ACCEPTANCE
ACCEPTANCE (*10[-1])
1.00
.75
.50
.25
0.00
0.00
3.00
6.00
9.00
12.00
15.00
18.00
MASS (GEV)

FIG. 2

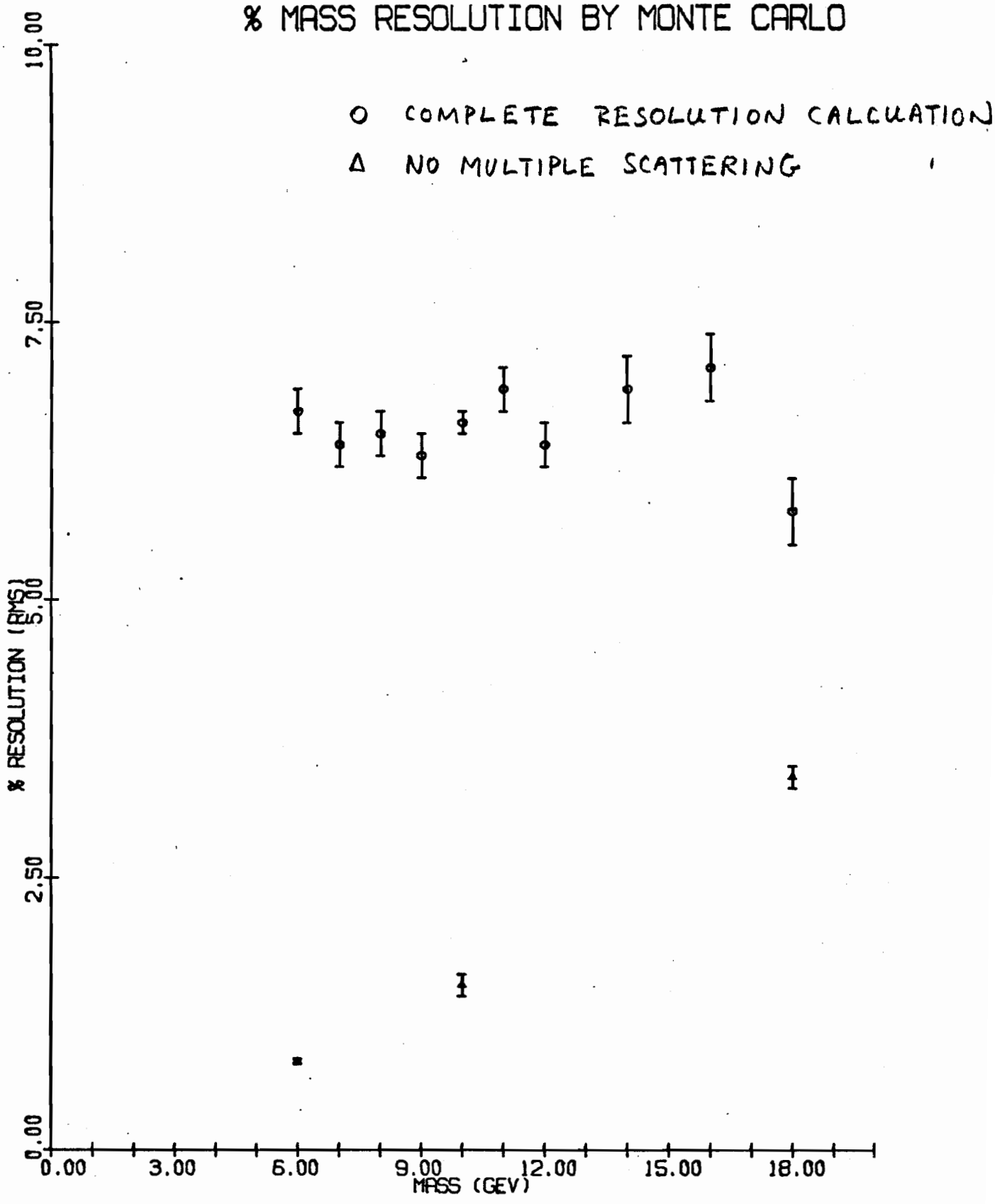
% MASS RESOLUTION BY MONTE CARLO
O COMPLETE RESOLUTION CALCULATION
Δ NO MULTIPLE SCATTERING
% RESOLUTION (RMS)
10.00
7.50
5.00
2.50
0.00
0.00
3.00
6.00
9.00
12.00
15.00
18.00
MASS (GEV)

FIG. 3

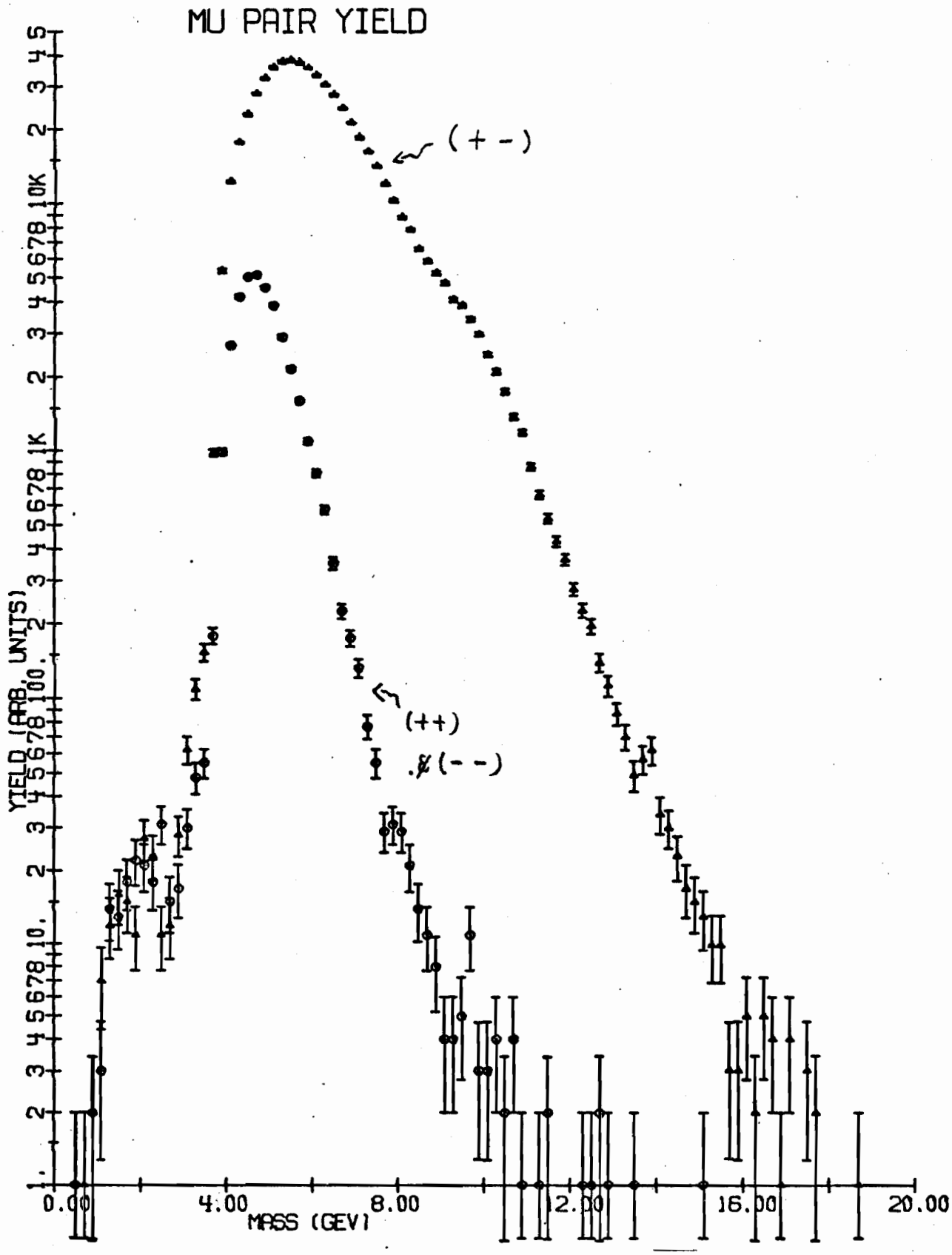
MU PAIR YIELD
YIELD (ARB. UNITS)
1. 2 3 4 5 6 7 8 10. 2 3 4 5 6 7 8 100. 2 3 4 5 6 7 8 1K 2 3 4 5 6 7 8 10K 2 3 4 5
(+ -)
(++)
(- -)
0.00
4.00
8.00
12.00
16.00
20.00
MASS (GEV)

FIG. 4

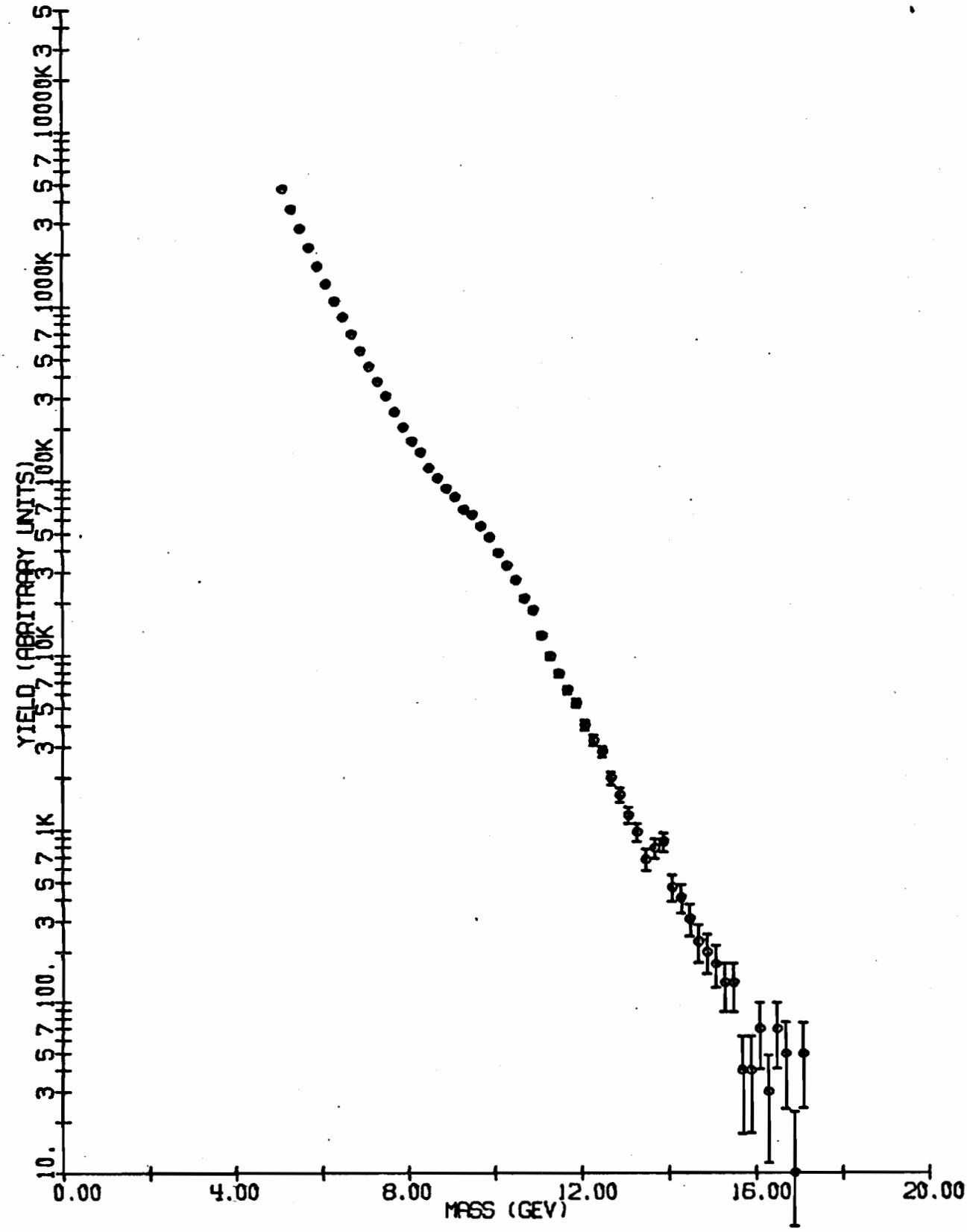
RESULTS(8/13/78) MNWT COLLABORATION FERMILAB EXP. 439
YIELD (ARBITRARY UNITS)
10.
100.
1K
10K
100K
1000K
10000K
0.00
4.00
8.00
12.00
16.00
20.00
MASS (GEV)

FIG. 5

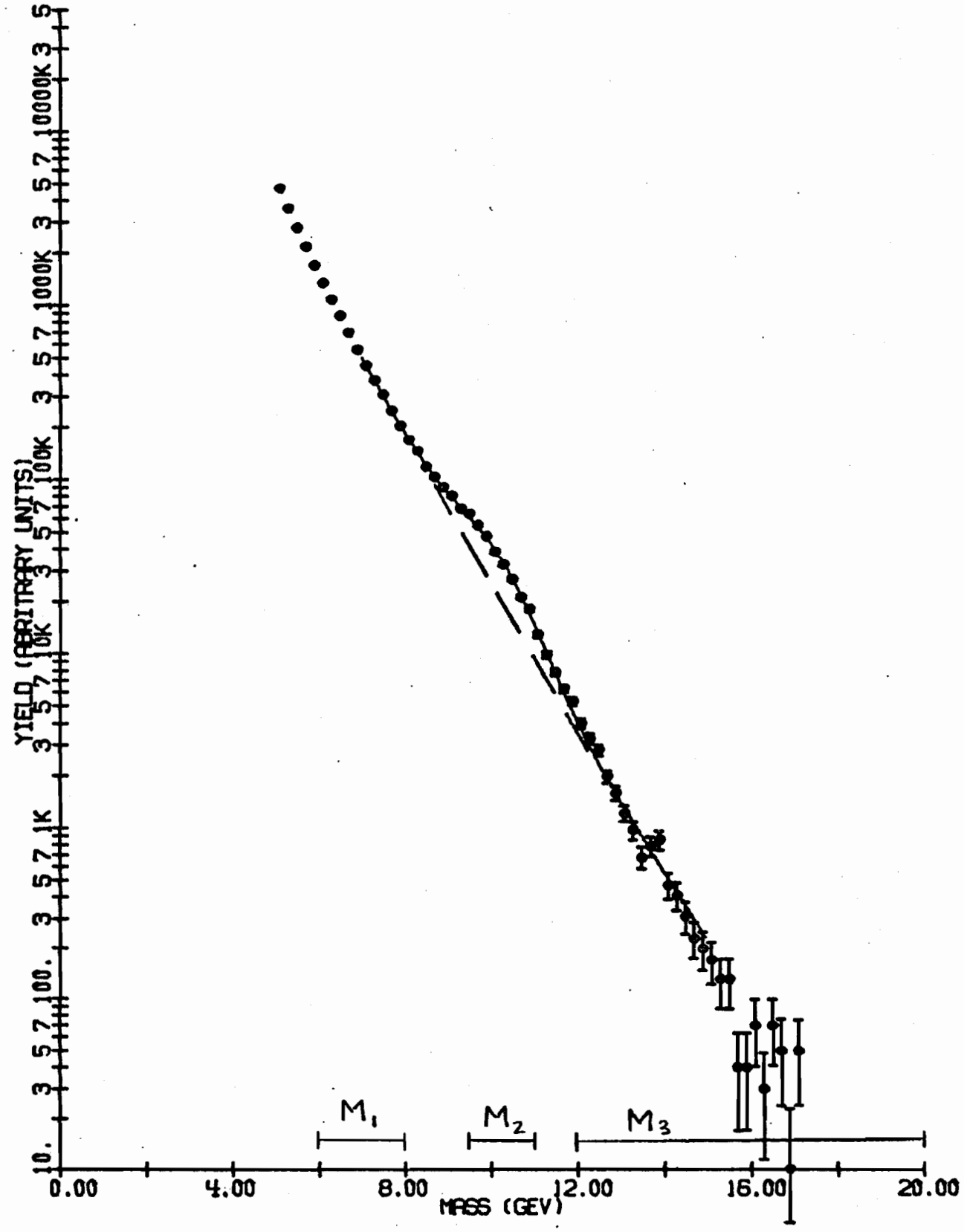
RESULTS(8/13/78) MNWT COLLABORATION FERMILAB EXP. 439
YIELD (ARBITRARY UNITS)
10.
100.
1K
10K
100K
1000K
10000K
0.00
4.00
8.00
12.00
16.00
20.00
MASS (GEV)
M1
M2
M3

FIG.6

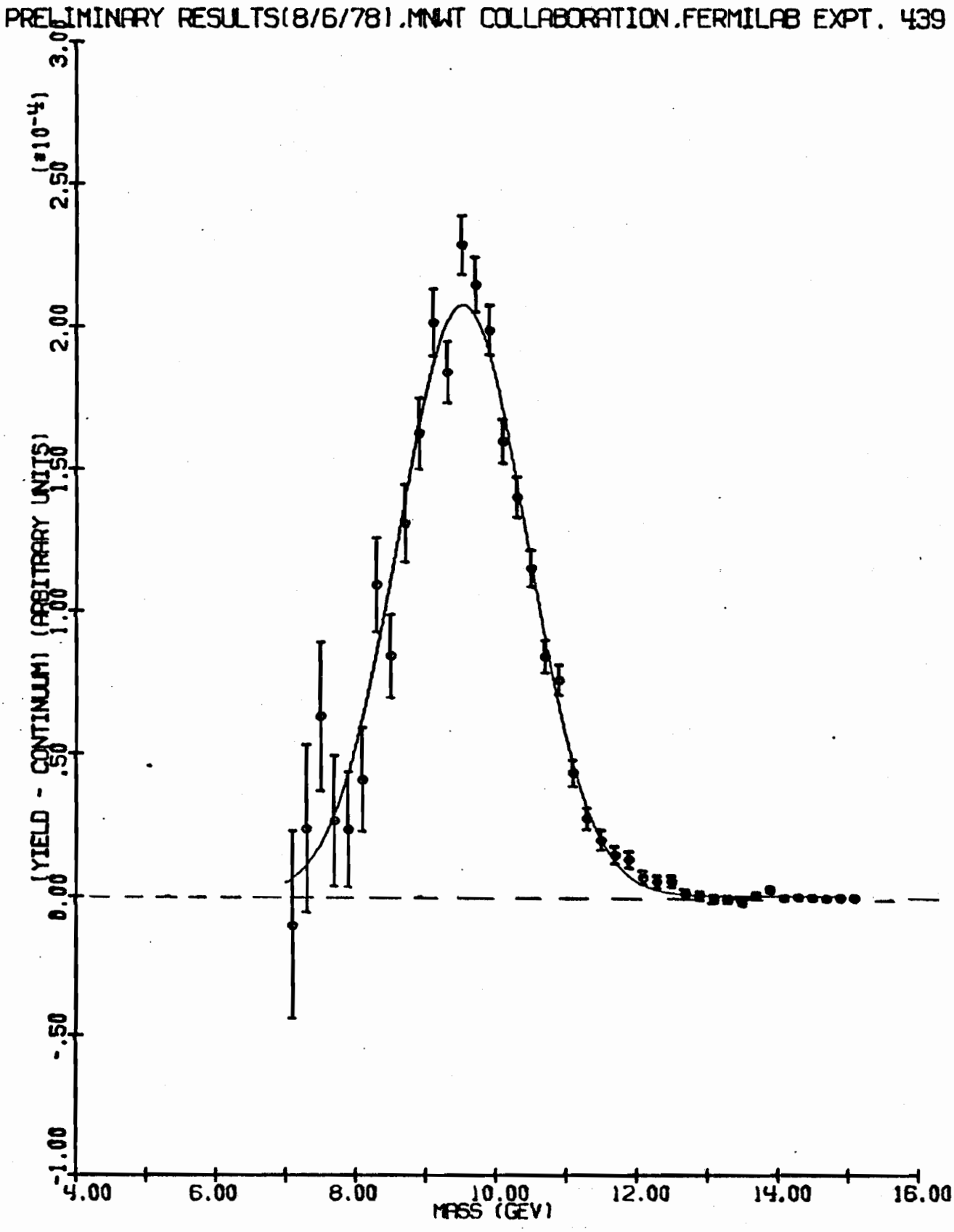
PRELIMINARY RESULTS(8/6/78).MNWT COLLABORATION.FERMILAB EXPT. 439
(YIELD - CONTINUUM) (ARBITRARY UNITS)
(*10**-4)
3.00
2.50
2.00
1.50
1.00
.50
0.00
-.50
-1.00
4.00
6.00
8.00
10.00
12.00
14.00
16.00
MASS (GEV)

FIG. 7

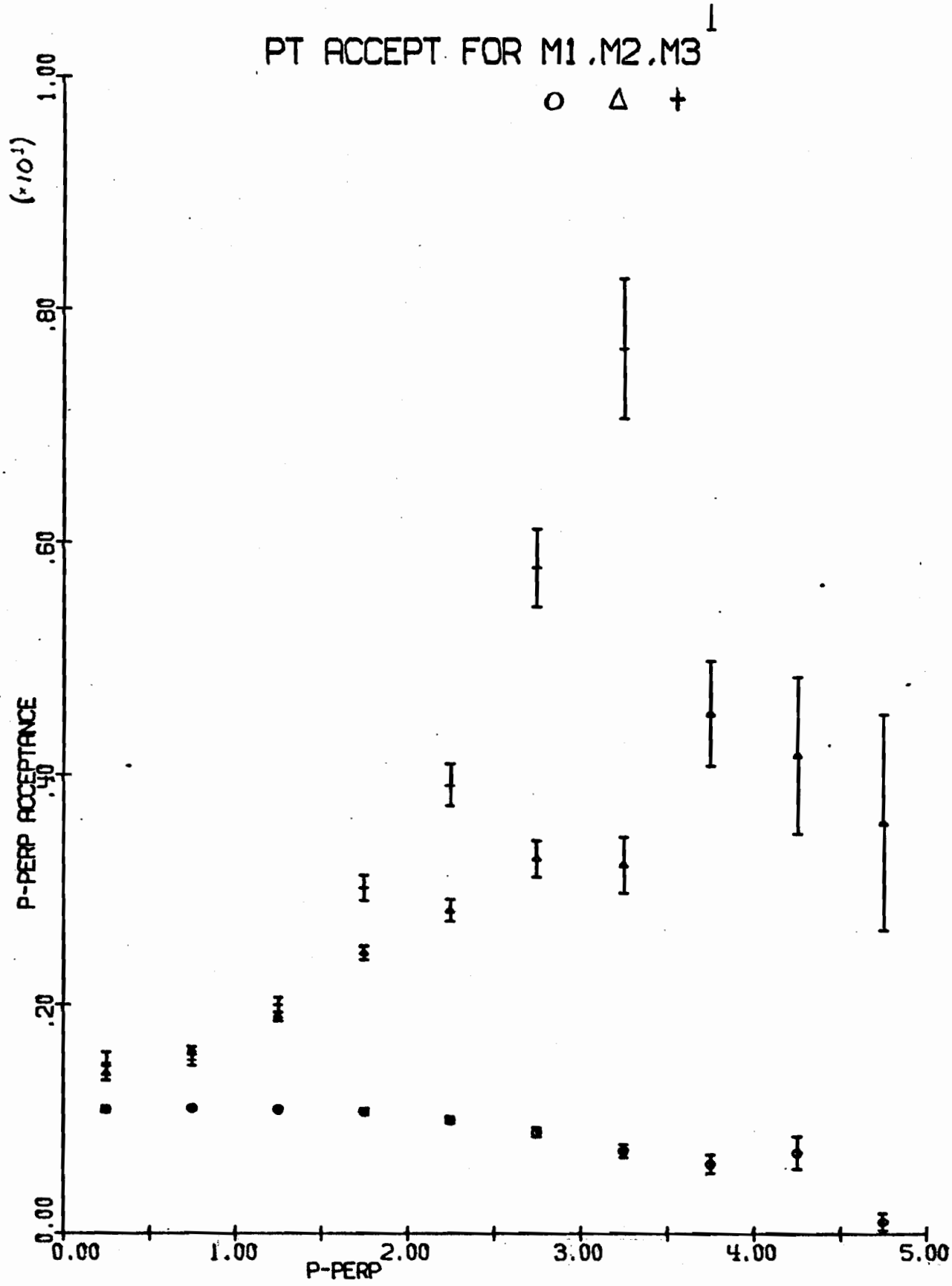
PT ACCEPT FOR M1.M2.M3
o Δ +
(*10⁻¹)
P-PERP ACCEPTANCE
1.00
.80
.60
.40
.20
0.00
0.00
1.00
2.00
3.00
4.00
5.00
P-PERP

FIG.8

P-PERP DISTRIBUTION

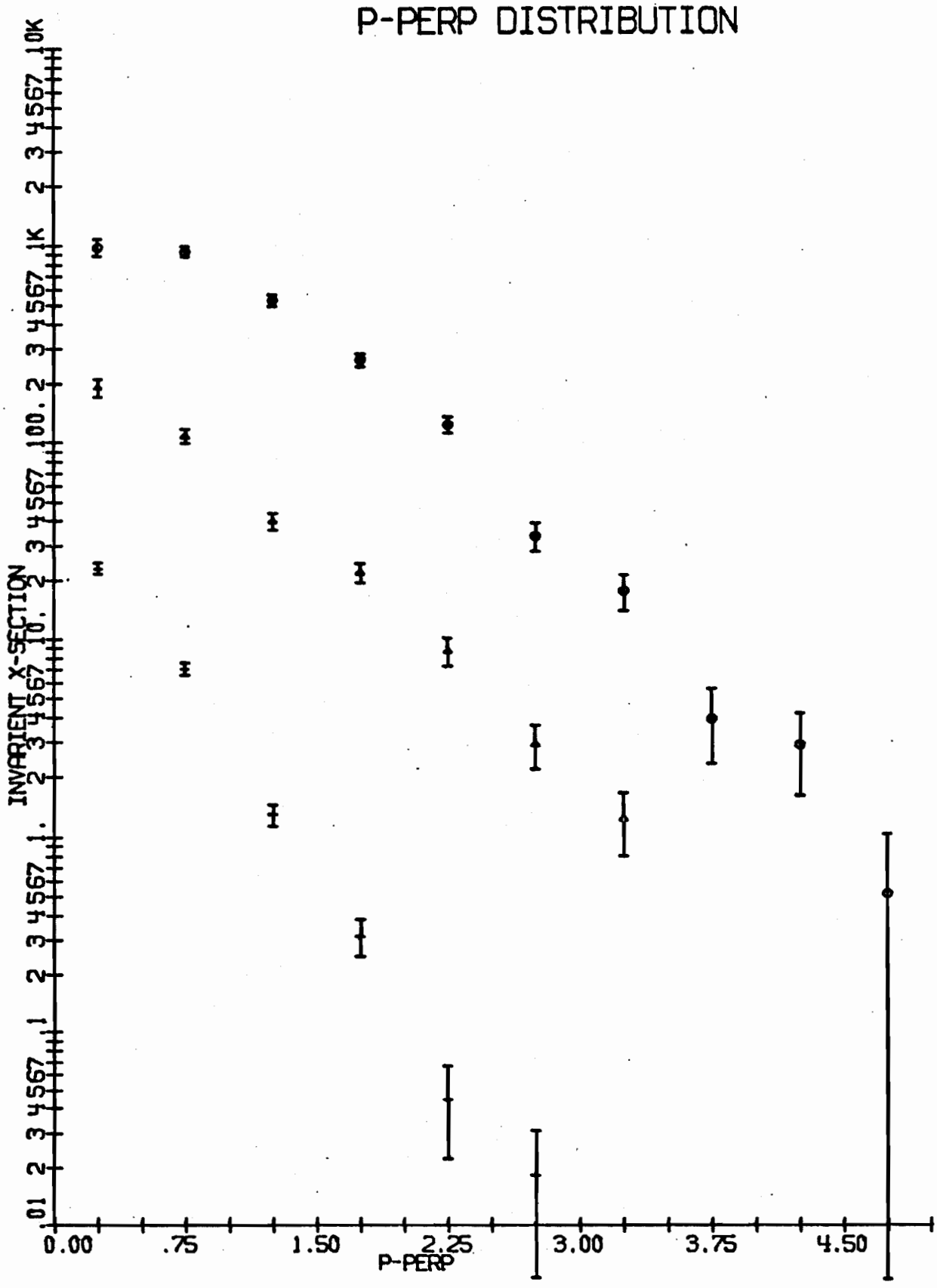

FIG. 9

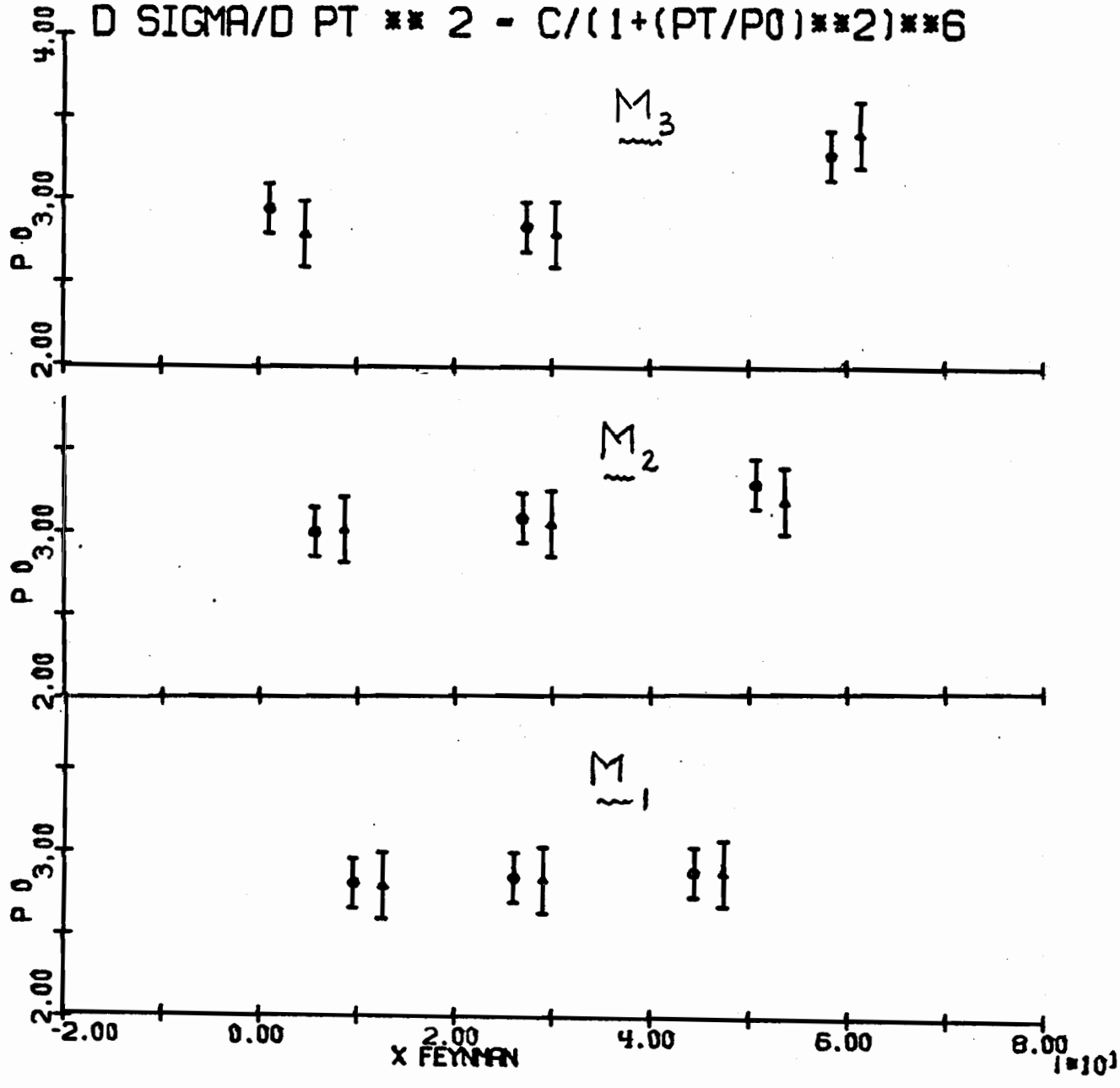
D SIGMA/D PT ** 2 - C/(1+(PT/P0)**2)**6
M3
M2
M1
P0
4.00
3.00
2.00
-2.00
0.00
2.00
4.00
6.00
8.00
X FEYNMN
(*10)

FIG. 10

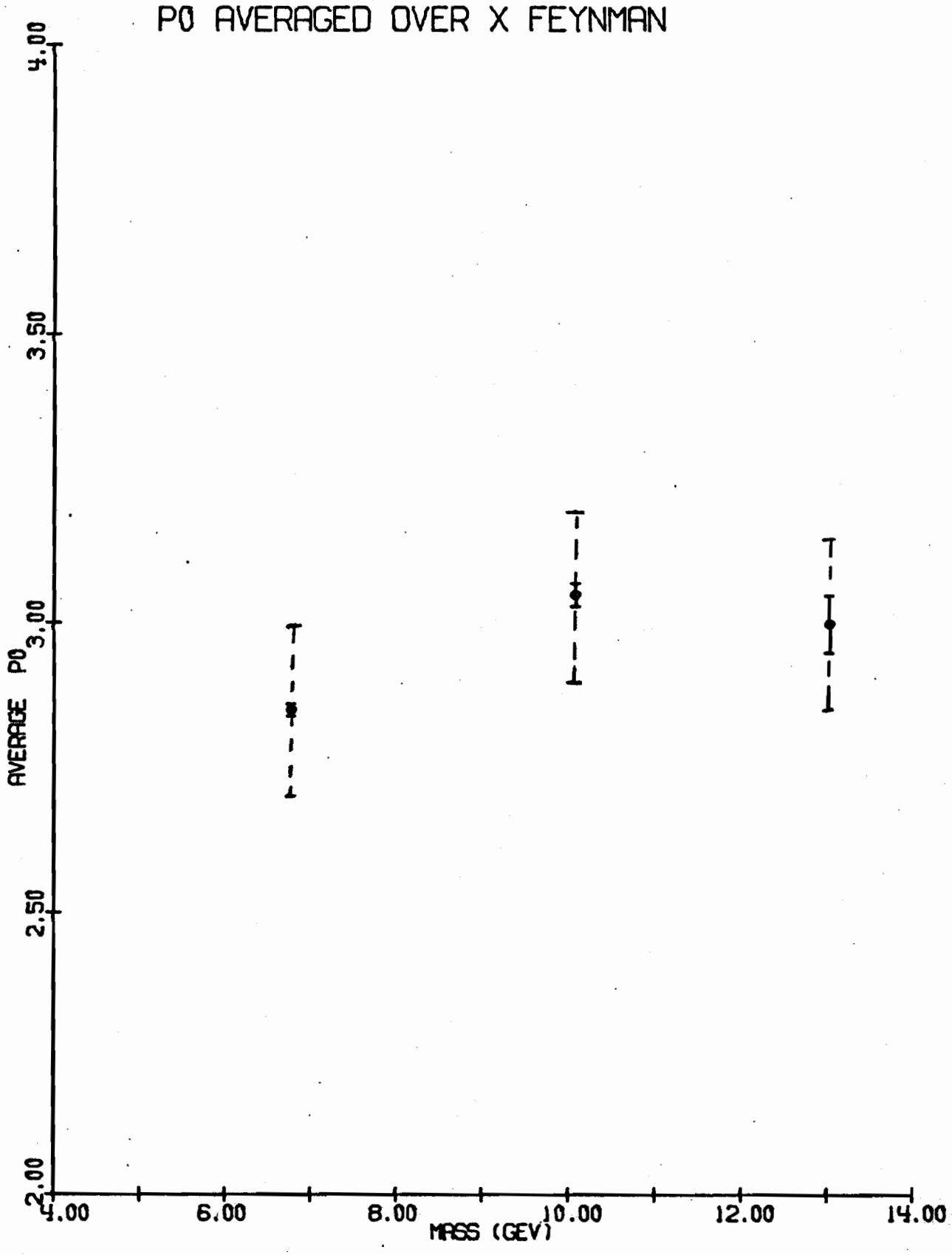
P0 AVERAGED OVER X FEYNMAN
AVERAGE P0
4.00
3.50
3.00
2.50
2.00
4.00
6.00
8.00
10.00
12.00
14.00
MASS (GEV)

FIG. 11

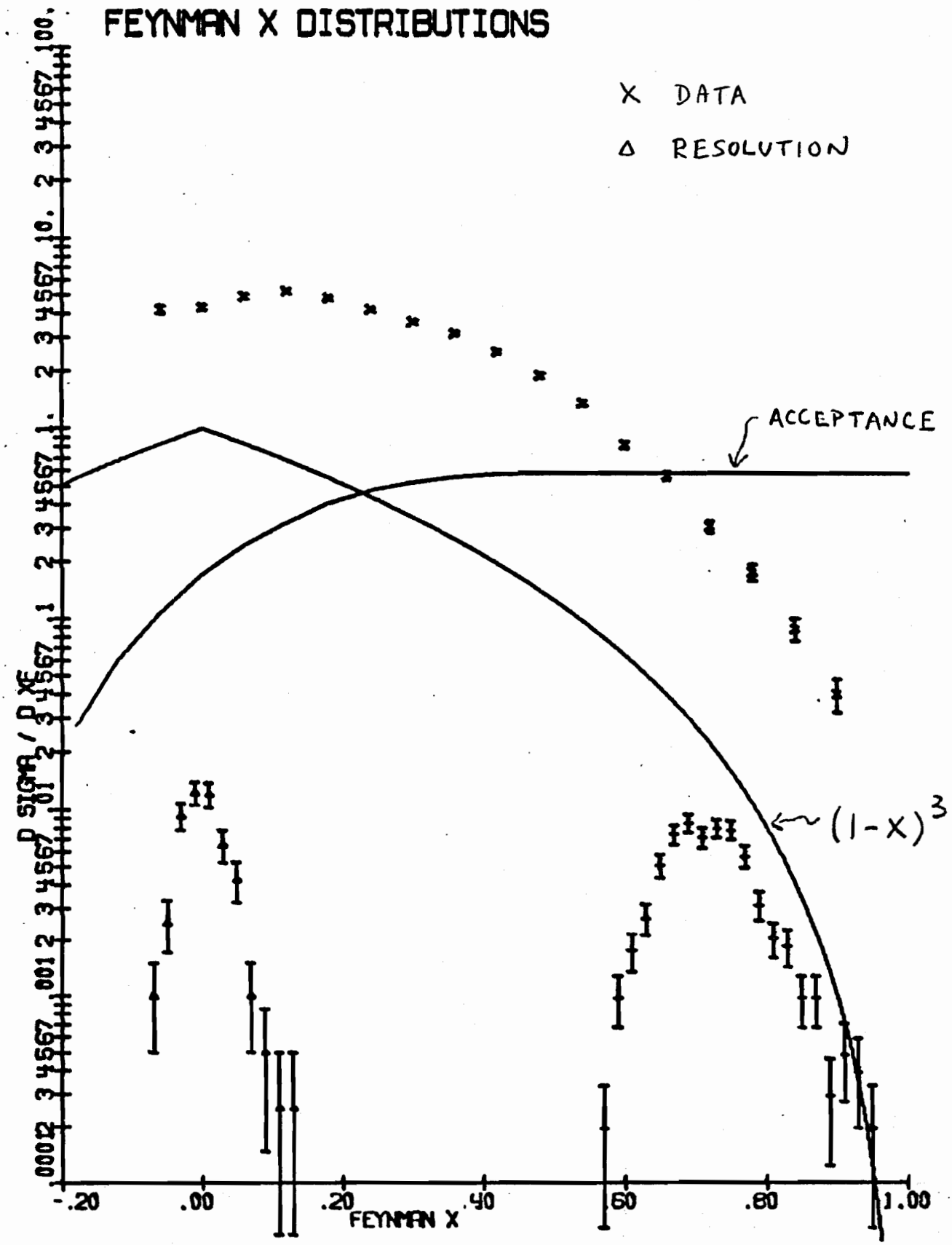
FEYNMAN X DISTRIBUTIONS
X DATA
Δ RESOLUTION
ACCEPTANCE
$(1-X)^3$
D SIGMA / D XF
FEYNMAN X
-.20
.00
.20
.40
.60
.80
1.00

FIG. 12

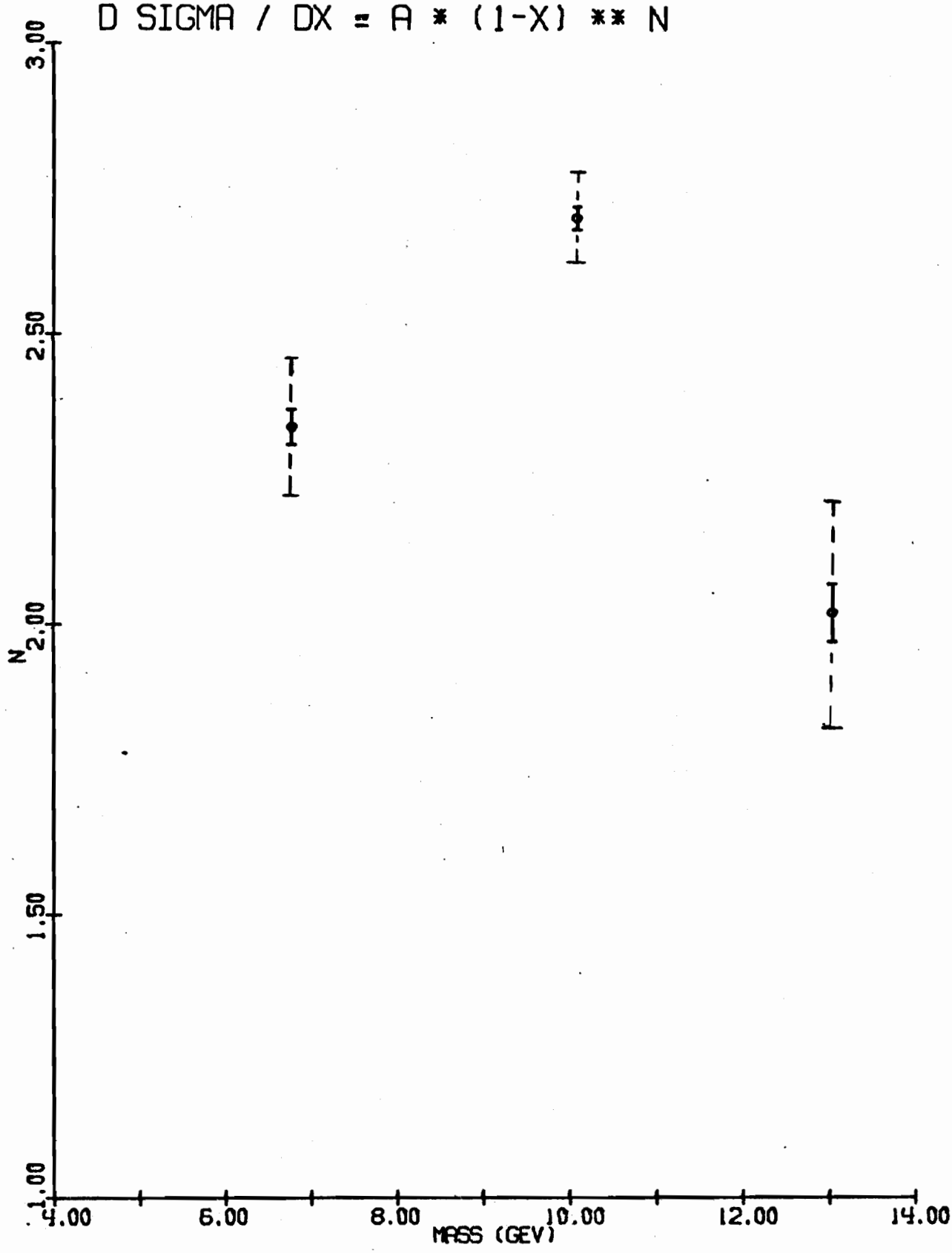
D SIGMA / DX = A * (1-X) ** N
3.00
2.50
2.00
1.50
1.00
N
4.00
6.00
8.00
10.00
12.00
14.00
MASS (GEV)

FIG. 13

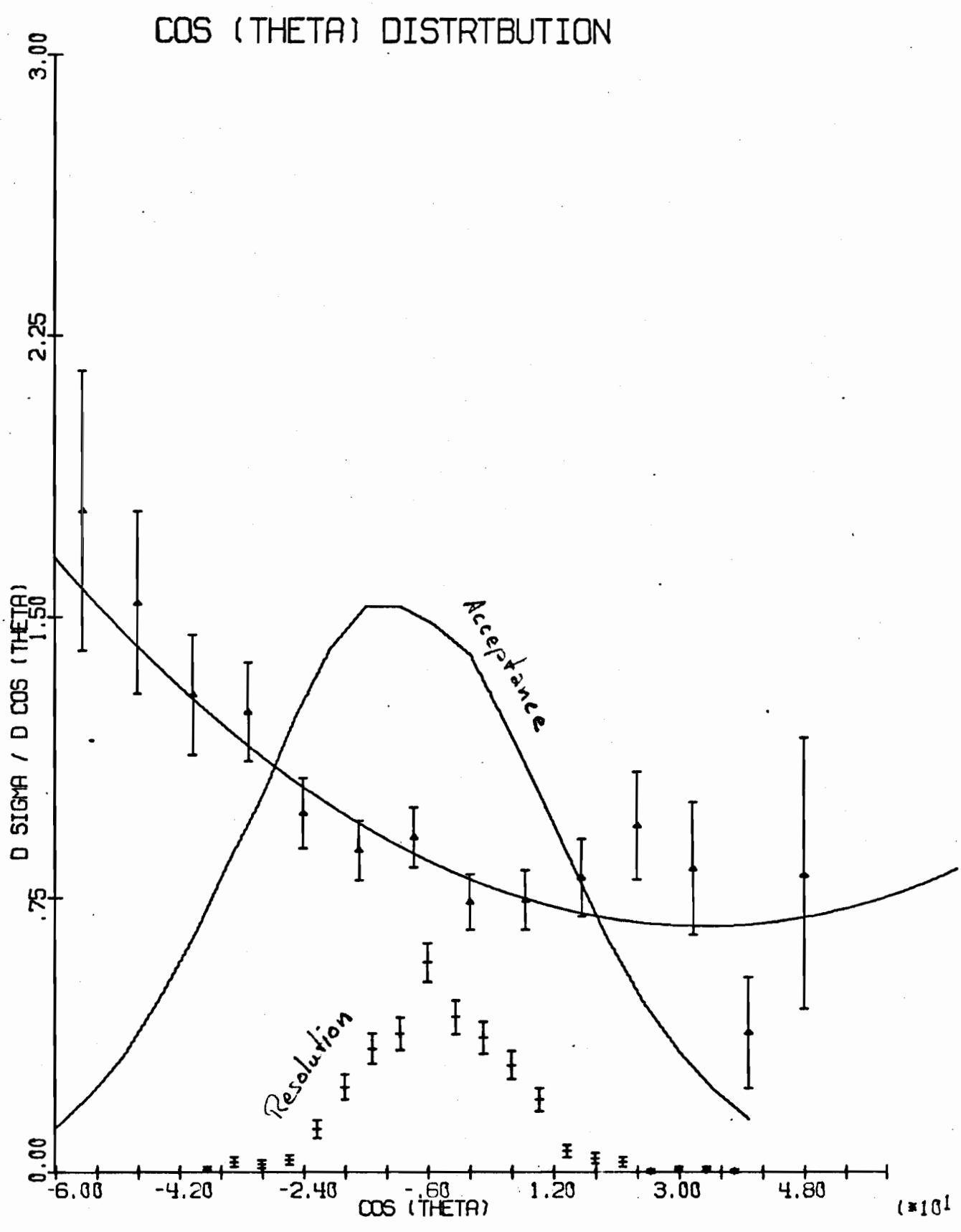
COS (THETA) DISTRTBUTION
D SIGMA / D COS (THETA)
3.00
2.25
1.50
.75
0.00
Acceptance
Resolution
-6.00
-4.20
-2.40
-.60
1.20
3.00
4.80
COS (THETA)
(*10¹

FIG. 14

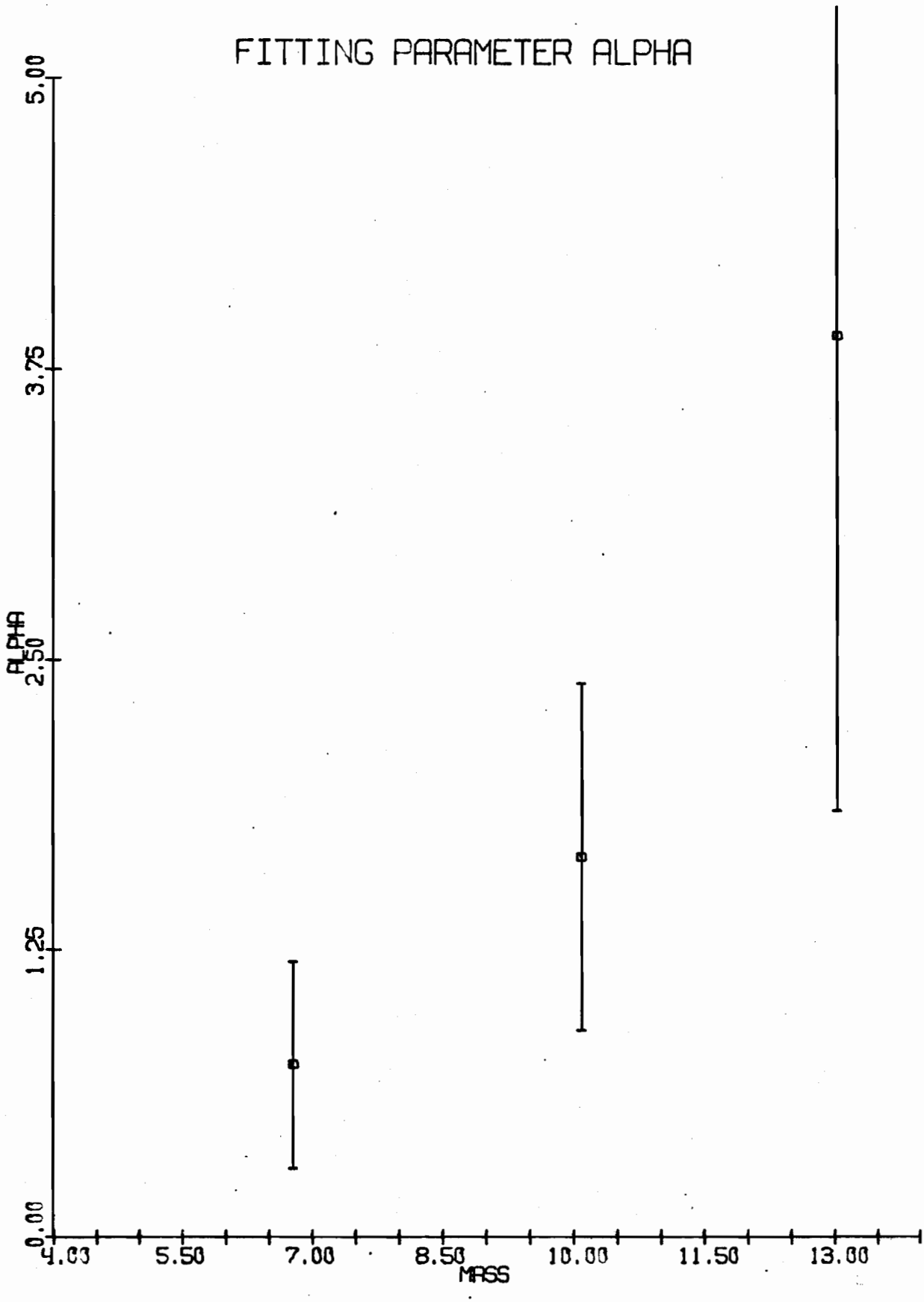
FITTING PARAMETER ALPHA
ALPHA
5.00
3.75
2.50
1.25
0.00
4.00
5.50
7.00
8.50
10.00
11.50
13.00
MASS